



Chlorine dioxide gas generation using rotating packed bed for air disinfection in a hospital

Viet Minh Trinh^a, Min-Hao Yuan^b, Yi-Hung Chen^{a,*}, Chen-Yang Wu^a, Shao-Chi Kang^a, Pen-Chi Chiang^c, Ta-Chih Hsiao^c, Han-Pang Huang^d, Yu-Lin Zhao^d, Ji-Fan Lin^e, Chien-Hsien Huang^{f,h}, Jiann-Horng Yeh^{g,h}, Der-Ming Leeⁱ

^a Department of Chemical Engineering and Biotechnology, National Taipei University of Technology, Taipei, 106, Taiwan

^b Department of Occupational Safety and Health, China Medical University, Taichung, 406, Taiwan

^c Graduate Institute of Environmental Engineering, National Taiwan University, Taipei, 106, Taiwan

^d Department of Mechanical Engineering, Center for Artificial Intelligence and Robotic, National Taiwan University, Taipei, 106, Taiwan

^e Department of Research, Shin Kong Wu Ho-Su Memorial Hospital, Taipei, 111, Taiwan

^f Department of Infection, Shin Kong Wu Ho-Su Memorial Hospital, Taipei, 111, Taiwan

^g Education and Research, Shin Kong Wu Ho-Su Memorial Hospital, Taipei, 111, Taiwan

^h College of Medicine, Fu Jen Catholic University, Hsinchuang, Taipei, 242, Taiwan

ⁱ Leaderman Environmental Technology Co., Ltd., Taipei, 110, Taiwan

ARTICLE INFO

Handling editor: Panos Seferlis

Keywords:

Rotating packed bed
Air stripping
Chlorine dioxide
Air disinfection
E. coli
G. stearothermophilus

ABSTRACT

Chlorine dioxide (ClO_2) has proven its efficiency as a fumigant toward bacteria and viruses. However, it still has challenges on its portability and simplicity of ClO_2 generation to meet the demand for disinfection in public and medical sectors. In this study, ClO_2 stripping process via a rotating packed bed (RPB) from the commercial ClO_2 solution was developed to a non-chemical-reaction ClO_2 generation for air sterilization in a hospital. The ClO_2 stripping efficiency (η) and the volumetric liquid mass-transfer coefficient ($K_L a$) were examined under various operating variables, such as initial liquid concentration (C_{Li}), rotational speed (ω), gas-to-liquid flow rate ratio (Q_G/Q_L), and liquid flow rate (Q_L). The results indicated that the gaseous ClO_2 can be rapidly and continuously generated via stripping using RPB with η varied above 97% in the certain range of C_{Li} (100–2000 mg/L) and Q_L (0.04–0.250 L/min). The overall $K_L a$ depends on the change of Q_L and ω , varied from 0.009 s^{-1} to 0.027 s^{-1} . The output concentration of gaseous ClO_2 (C_G) can be adjusted from around 10 ppm to over 1000 ppm based on the established prediction model and controlling C_{Li} , Q_L , Q_G , and ω . The results of the on-site disinfection test in the *Mycobacterium Tuberculosis* Laboratory in a hospital have shown effective elimination of all sites of *E. coli* and 2 of 5 sites of *G. stearothermophilus* with a C_T value at the gas monitoring point of 642 ppm-h and humidity of 81%.

1. Introduction

On March 11, 2020, the World Health Organization has declared the coronavirus disease 2019 (COVID-19) as a global pandemic (WHO, 2020). One main reason for the dramatic worldwide spread is its 2–14 days of incubation period in the human body, which leads to an asymptomatic and subclinical infection among people unexpectedly (Jiang et al., 2020). Since the SARS-CoV-2 can last on different materials for varying amounts of time, contaminated surfaces were considered as a pathway of indirect contact transmission (Suman et al., 2020). Hence, the demand for disinfection for hospitals and disease control centers also

upsurged as a result. Fumigation is a traditional method for disinfection of closed areas. Several oxidative chemicals, such as ozone (O_3), chlorine (Cl_2), hypochlorous acid (HOCl), chlorine dioxide (ClO_2), and hydrogen peroxide (H_2O_2), were employed to inactivated influenza virus and human noroviruses in the contaminated surface and public sectors (Khan and Yadav, 2020; Lu et al., 2021). Among them, HOCl and ClO_2 are well known for their strong oxidation effect for antimicrobial activity against pathogens, such as bacterial, fungi, and viruses (Shirasaki et al., 2016). HOCl is commonly used by aqueous form via fogging machine or wipes for disinfection. Note that 100 ppm of sprayed HOCl with a 20-min exposure was sufficient to reduce 99.5% of *Staphylococcus*

* Corresponding author.

E-mail address: yhchen1@ntut.edu.tw (Y.-H. Chen).

<https://doi.org/10.1016/j.jclepro.2021.128885>

Received 5 May 2021; Received in revised form 14 August 2021; Accepted 30 August 2021

Available online 2 September 2021

0959-6526/© 2021 Elsevier Ltd. All rights reserved.

epidermidis (Okamoto et al., 2019). However, the fogging process of HOCl may result in evaporation of chlorine gas and safety concerns (Zhao et al., 2014). On the other hand, while aqueous ClO₂ has been successfully applied for drinking water disinfection instead of Cl₂ (Jiang et al., 2012), gaseous ClO₂ has been considered as a good option for closed room disinfection. According to Lowe et al. (2013), the inactivation ability of ClO₂ at a C_T value (the exposure concentration at a certain contacting period) around 600–800 ppm-h from the Minidox-M Decontamination System (Clordisys Solution, Inc.) exhibits 8 log reduction of various types of organism, such as *A. baumannii*, *E. coli*, *E. faecalis*, *M. smegmatis*, and *S. aureus*, and 9 out of 10 sites without the growth of bacillus atrophaeus biological indicator under the condition of relative humidity above 50% in a 20 m² biosafety level 3 laboratory of a hospital (Lowe et al., 2013). Theoretically, ClO₂ might leave some small amount of residual such as free ClO₂, chlorate (ClO₃[−]), and chlorite (ClO₂[−]) on the surface after disinfection by both aqueous and gaseous forms. These residual/layers of chemicals might remain for hours based on their surrounding temperature and humidity condition. However, a food sanitization study showed that 100 mg/L of ClO₂ solution was able to achieve 3–5 log reduction of *E. coli*, *Listeria*, and *Salmonella* with a very low concentration of ClO₂ and satisfying the US EPA standard for drinking water (Trinetta et al., 2011).

The generation of gaseous ClO₂ involves the oxidation of chlorite (ClO₂[−]), which is mostly derived from the reaction scheme of chlorine-sodium chlorite and acid-sodium chlorite (Ran et al., 2019; Shirasaki et al., 2016). Several gaseous ClO₂ generators based on chlorine-sodium chlorite reactions have been investigated to produce a high concentration for industrial applications. The Cl₂ gas firstly reacts with H₂O to form HOCl and HCl. These acids then react with sodium chlorite (NaClO₂) to form ClO₂, NaCl, and H₂O. In the chlorine-sodium chlorite reaction system, the ratio between Cl₂ gas and NaClO₂ should be well controlled since excess Cl₂ will lead to the formation of sodium chlorate (NaClO₃) rather than ClO₂. This method has been proven to generate a high concentration of ClO₂ with a high reaction rate and yield. However, the drawbacks of a careful balance of Cl₂/NaClO₂ ratio and safety concern of the extra-compartment for Cl₂ gas would restrict its feasibility for the application in the public and medical sectors. In reaction conditions of 3–5% Cl₂ gas-air mixture through a column containing 500 g of NaClO₂ chips over 30 min, the gaseous concentration of ClO₂ can reach 7–30 mg/L (about 2500–10000 ppm) (Jeng and Woodworth, 1990). Eylath et al. (2003) also employed the commercial plastic cartridges containing NaClO₂ (CD-Cartridge set, ClorDiSys solution, Inc.) perfused by 2% Cl₂–98% N₂ mixture to generate gaseous ClO₂ at the concentration of around 5–7.5 mg/L (1800–2700 ppm) over 60 min (Eylath et al., 2003). On the other hand, the reaction of acid-sodium chlorite was employed in several lab-scale research due to its simplicity and easy operation (Ran et al., 2019). In this method, NaClO₂ reacts directly with an acid (HCl, H₂SO₄, H₃PO₄) to produce ClO₂, sodium salt, and H₂O. This reaction only requires sufficient acid without controlling the balance of reactants to generate ClO₂ product. However, the ClO₂ yield of this scheme is relatively lower than that of the chlorine-sodium chlorite reaction. Shirasaki et al. (2016) directly mixed 3.35% NaClO₂ solution with 85% phosphoric acid in a testing chamber and gradually generated ClO₂ to the peak concentration of 40 ppm in the closed room of 87 m³ after 2 h and 20 mL/m³ (Shirasaki et al., 2016). The production efficiency would also depend on the ambient conditions such as temperature and humidity. Li et al. (2012) showed that the gaseous ClO₂ from sodium direct reaction between NaClO₂ and solid acid required considerable time and uncontrollable output concentration (Li et al., 2012). Therefore, the limitations of the acid-sodium chlorite reaction scheme are lower yield rate, lower and uncontrollable output gas concentration with longer reaction time to reach maximum yield in comparison to the chlorine-sodium chlorite reaction.

Gaseous ClO₂ is unstable and potentially explosive when the concentration greater than 10% (Chen et al., 2020). Therefore, the industrial ClO₂ product tends to be stored in form of a liquid solution by

low-temperature absorption up to 8 g/L at 30 °C and easily separated from liquid phase to gas phase. The suitable approach for ClO₂ solution preservation is to store in a well-sealed bottle at a low temperature, which may restrict the accessibility and feasibility for its disinfection practice. To tackle this issue, instant chlorine dioxide effervescent tablets were commercially developed to obtain the desired ClO₂ solution on-site by dissolving the tablets into water (Zhang, 2011).

The gaseous ClO₂ can be stripped out by counter-currently passing the airflow through the ClO₂ solution inside a packed bed (Chen et al., 2020). Hence, it is possible to generate a favored dosage of ClO₂ via air stripping since the outlet concentration of gas ClO₂ can be adjusted by inlet liquid flowrate and gas flowrate. Regarding air stripping devices, the rotating packed bed (RPB) has shown a promising performance with its high mass transfer efficiency, low retention time, and small compact equipment size. The air stripping of VOCs from groundwater (Gudena et al., 2011; Singh et al., 1992), stripping of ethanol (Liu et al., 1996), and stripping of ammonia (Yuan et al., 2016a, b), were conducted by the RPB. Gudena et al. (2011) showed that a small-size RPB (HiGee Stripper, inner radius = 0.04 m, outer radius = 0.52 m, height = 0.64 m) achieved a similar VOC stripping efficiency of 98.63% from groundwater with that of much-larger-size conventional column (diameter = 1.5 m, tower height = 9.2 m, packing height = 5.5 m) at the same hydraulic loading of 0.04 m³/s (Gudena et al., 2011). This intensified mass transfer, which leads to the smaller size required for the equipment, is the result of high centrifugal force (300–10,000 m/s²) that is 1–3 order of magnitude greater than gravitational acceleration (Cortes Garcia et al., 2017). Yuan et al. (2016a) compared the performance between the RPB and other conventional stripping devices (stripping tanks, packed towers, and other advanced gas–liquid contactors) in air stripping of ammonia wastewater. The findings revealed that the RPB exhibits a stronger mass-transfer performance (12.3–18.4 1/h) and shorter retention time (0.0037 h) compared with those of the conventional devices (0.42–1.2 1/h and 3.5–9 h) (Yuan et al., 2016a). Therefore, a higher gas-liquid mass transfer with significantly reduced retention time and equipment size would lead to lower the and capital cost compared to these conventional columns.

While chemical-reaction-type ClO₂ gas generators are still challenged to be employed for air disinfection in public and medical sectors, this study focuses on the stripping of ClO₂ with an RPB equipment as a non-chemical-reaction ClO₂ generator to generate the fumigant for air sterilization. ClO₂ effervescent tablets were used to prepare the stock solution on-site. Once the tablets were completely dissolved, the stripping process was carried out immediately to avoid the expected decay in ClO₂ solution concentration. The experimental variables of initial liquid concentration (C_{Li}), rotational speed (ω), liquid flow rate (Q_L) and gas-to-liquid flow rate ratio (Q_G/Q_L) were adopted to examine their effects on the gas-phase concentration (C_G), stripping efficiency (η) and overall liquid volumetric mass transfer coefficient (K_{La}) for ClO₂ stripping via RPB. The prediction models of C_G, η, and K_{La} were also established based on the theoretical and empirical considerations. Furthermore, the disinfection experiment using gaseous ClO₂ generated from the RPB was performed in a *Mycobacterium Tuberculosis* Laboratory of a hospital to determine the inactivation efficiency toward *E. coli* and the biological indicator of spores (*Geobacillus stearothermophilus*) at a certain C_T value. The findings would be beneficial for the development and employment of a safer and intensified stripping process via a non-chemical-reaction method of controllable ClO₂ generation for air disinfection in a hospital.

2. Material and methods

2.1. ClO₂ Stripping experiment

2.1.1. The ClO₂ gas generator

The ClO₂ gas generator (Model 00024-S100210, HiGee Co. Ltd., New Taipei City, Taiwan), composes of SUS 304 RPB, liquid distributor, and packing material of stainless-steel wire mesh, was used for generating

continuous and stable ClO_2 concentration in gas-phase, as shown in Fig. 1. This system is equipped with an diaphragm liquid pump (NFH200, Nikkiso Eiko, Tokyo, Japan) to maintain the continuous feeding of ClO_2 solution. An air blower (Model YHS, Yung Hsing Machine and Electric Industrial Co., Ltd, Taichung, Taiwan) which is controlled by a frequency adjuster (Model VFD-S1, Delta, Taipei, Taiwan) is responsible for the stable air supply. The gas flow rate was monitored by an anemometer (Model FY856, Huizhou FUYI Electronic Technology Co., Ltd., Huizhou, Guangdong, China). All the parts are firmly assembled in a stainless-steel cast with an electrical control panel. The properties of the RPB are listed in Table 1.

2.1.2. Experimental procedure and conditions

A schematic diagram of ClO_2 stripping by the RPB is shown in Fig. 2. The stock ClO_2 solution was prepared by dissolving the commercial ClO_2 effervescent tablets (Green Disinfectant, Virashield Asia Limited, Hong Kong, China) with deionized water. Diluting one effervescent pallet into 1 L can produce about 100 ppm ClO_2 solution with the pH value of 2.30. The stripping process was performed in a continuous-flow mode with constant liquid and air injection.

In this study, the effects of initial liquid concentration (C_{Li}) of 160–1730 mg/L, rotational speed (ω) of 900–1500 rpm, gas-to-liquid flow rate ratio (Q_G/Q_L) of 1000–10000, and liquid flow rate (Q_L) of 0.040–0.210 L/min on the gas-phase concentration (C_G), stripping efficiency (η), and overall liquid volumetric mass transfer coefficient (K_La) were comprehensively examined for ClO_2 stripping via RPB. The C_{Li} were controlled by the dosage of the tablets. The effect of Q_G/Q_L was assessed at a constant Q_L at 0.092 L/min, while the Q_G was changed by 100–1000 L/min. The Q_L was adjusted at various stages from 0.040 to 0.210 L/min while the Q_G was set from 100 to 1000 L/min (corresponded to the gas velocity of 1–8 m/s at the diameter of 0.0512 m of the gas tube). For each experimental condition, duplicate tests were performed and sampled after 15 min of the stripping process to reach a

Table 1

Properties of the RPB for ClO_2 stripping.

Item (Unit)	Value
Inner radius of a packed bed (r_i) (m)	0.0290
Outer radius of a packed bed (r_o) (m)	0.0745
Average radius of a packed bed (r_{avg}) (m)	0.0518
Axial height of a packed bed (Z_B) (m)	0.050
Volume of a packed bed (V_B) (m^3)	7.39×10^{-4}
Packing material	Stainless-steel wire mesh
Specific area of a packing per unit volume of a packed bed (a_p) (m^2/m^3)	840
Total packing area ($a_p \cdot V_B$) (m^2)	0.621
Voidage (ϵ) (m^3/m^3)	0.956

steady flow.

2.1.3. Analytical method

The dissolved ClO_2 in water was quantified by spectrophotometer equipment (Model Jasco V-730, JASCO Inc., Tokyo, Japan) and Beer's law calculation. The measurement of ClO_2 concentrations in the inflow (C_{Li}) and outflow (C_{Lo}) solutions was performed at the wavelength of 380 nm, where the molar absorptivity ϵ of ClO_2 at 380 nm is 837 L/mol-cm (Wang et al., 2011).

The concentration of gaseous ClO_2 (C_G) was measured by the ClO_2 Detector device (Model ATI Portasens II, Winsconsin, US) equipped with a ClO_2 sensor (Model 1/5 PPM 00–1020, ATI, Winsconsin, US) as well as calculated by the mass balance principle, as follows:

$$C_{Li}Q_L = C_{Lo}Q_L + C_GQ_G \quad (1)$$

From that the concentration of the ClO_2 in the outlet gas flow is calculated as:

$$C_G = \frac{(C_{Li} - C_{Lo}) \times Q_L}{Q_G} \left(\text{g} / \text{m}^3 \right) \times \frac{24.5 \text{ L/mol}}{67.45 \text{ mol/g}} \times 1000000 \text{ (ppm)} \quad (2)$$

in which 24.5 L/mol is the molar volume of gas in the standard laboratory condition, while 67.45 g/mol is the molar mass of ClO_2 . The measured C_G from the sensor and calculated C_G was mostly similar with the linear equation (data not shown, $R^2 = 0.9521$) as follow:

$$\text{Measured } C_G = \text{Calculated } C_G \times 1.0976 \quad (3)$$

2.1.4. Theoretical calculations

In this study, the stripping efficiency (η) was calculated from the ClO_2 concentration of the inlet (C_{Li}) and outlet (C_{Lo}) solution.

$$\text{Stripping efficiency } \eta(\%) = \frac{C_{Li} - C_{Lo}}{C_{Li}} \times 100\% \quad (4)$$

Based on the mass-balance principle and the two-film theory, the overall liquid volumetric mass transfer coefficient (K_La) was proposed by Singh et al. (1992) and Chen et al. (Chen et al., 2005a, b) to examine the performance of the rotating packed bed for ClO_2 stripping. This model was derived from the differential volume with the cross-sectional area and the thickness of the thin film with the assumption of neglecting gas-side mass transfer resistance (Lin et al., 2003). The expression for K_La calculation is as follows:

$$K_La = \frac{Q_L}{V_B} \frac{\ln \left[\left(1 - \frac{1}{S} \right) \frac{C_{Li}}{C_{Lo}} + \frac{1}{S} \right]}{1 - \frac{1}{S}} \quad (5)$$

where V_B is the volume of the packed bed, and S is the stripping factor defined as:

$$S = H_C \frac{Q_G}{Q_L} \quad (6)$$



Fig. 1. Photograph of the ClO_2 gas generator.

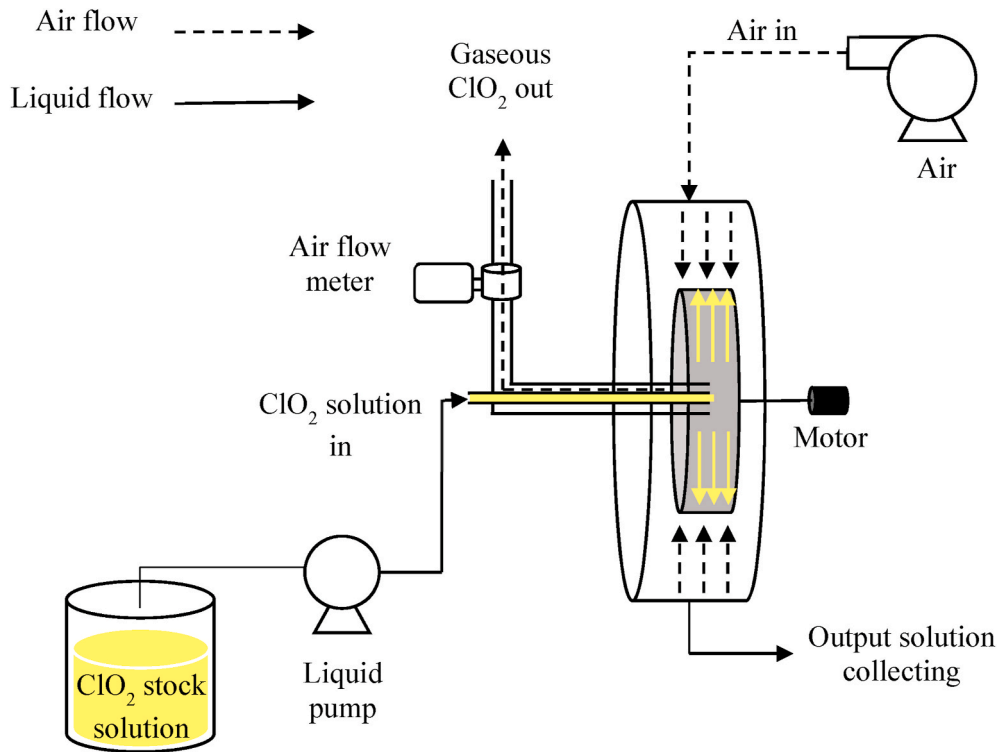


Fig. 2. A schematic diagram of ClO_2 gas generator.

where H_C ($H_C = 0.047696$) is the dimensionless Henry's law constant of ClO_2 at 30°C (NIST Chemistry WebBook).

The prediction models of η and $K_L a$ were also estimated for the comparison between the obtained experimental and theoretical values from the operating variables, dimensions of the RPB, and other gas and liquid properties, which were proposed by Kelleher and Fair (1996), Chen and Liu (2002), Chen et al. (2004), and Yuan et al. (Yuan et al., 2016a, b). To estimate the η and $K_L a$, the dimensionless groups of $Gr_{L,avg}$, Re_G , and Re_L was calculated from the ω , Q_G , and Q_L , respectively, as follows:

$$Gr_{L, avg} = \frac{r_{avg} \omega^2 (r_o - r_i)^3}{\nu_L^2} \quad (7)$$

$$Re_G = \frac{\rho_G Q_G \ln\left(\frac{r_o}{r_i}\right)}{2\pi Z_B (r_o - r_i) a_p \mu_G} \quad (8)$$

$$Re_L = \frac{\rho_L Q_L \ln\left(\frac{r_o}{r_i}\right)}{2\pi Z_B (r_o - r_i) a_p \mu_L} \quad (9)$$

The $K_L a$ then can be computed from these above dimensionless group as follows:

$$\frac{K_L a_p}{D_L a_p} = a \times Re_L^b Re_G^c Gr_{L,avg}^d \quad (10)$$

In which, d_p is the stainless-steel wire diameters of the packing (0.22), a_p is the specific area of packing per unit volume of the packed bed ($840 \text{ m}^2/\text{m}^3$). The D_L value is the molecular liquid diffusion coefficient of ClO_2 at 30°C ($1.43 \times 10^{-5} \text{ m}^2/\text{s}$) (US-EPA). The a , b , c , and d were power-law constants for the relation between experimental $K_L a$ and the dimensionless groups. Based on Eq. (5) and the predicted $K_L a$ from Eq. (10), Eq. (4) can be further modified as follows:

$$\eta = \left[1 - \frac{\left(1 - \frac{1}{S}\right)}{\exp\left(K_L a \frac{V_R}{Q_L} \left(1 - \frac{1}{S}\right)\right) - \frac{1}{S}} \right] \times 100\% \quad (11)$$

2.2. Disinfection experiment

2.2.1. Target microorganisms

The *Escherichia coli* (*E. coli*) and commercial biological indicator strip (Apex Biological Indicators, Mesa Lab, USA) preloaded with *Geobacillus stearothermophilus* were adopted for disinfection experiments. The *E. coli* was attached to porous beads and stored at -80°C . The beads were placed into blood agar plates and incubated at 37°C for 24 h. The colony density was adjusted to $6.3 \times 10^9 \text{ CFU/mL}$ and stored at 4°C before use. The biological indicator strip with 10^6 spores of *Geobacillus stearothermophilus* was employed to validate the disinfection ability of gaseous ClO_2 fumigation. The exposed groups and non-exposed (control) groups were set for the experiments of *E. coli* and *Geobacillus stearothermophilus*. The exposed and non-exposed *Geobacillus stearothermophilus* samples were then taken to an 8-h of incubation to observe the change in color to determine the color change which indicates the inactivation efficiency of ClO_2 . The log reduction and disinfection efficiency toward *E. coli* were determined by comparison of the survival of the population with that in the control group.

2.2.2. Testing room and operational condition

To assess the disinfection ability of gaseous ClO_2 generated from the RPB, the *M. Tuberculosis* Laboratory of Shin Kong Wu Ho-Su Memorial Hospital (Taipei, Taiwan) was set as an on-site testing room for the disinfection experiment. The floor plan of the laboratory and its dimension is presented in Fig. 3, which has a height of 2.268 m and a space volume of 30.6 m^3 . The RPB-CDGG12 was put outside the window of *M. Tuberculosis* Lab with a port to inject the generated gaseous ClO_2 . Two circulation fans were used to provide high diffusion and distribution of gaseous ClO_2 in the chamber throughout the experiment.

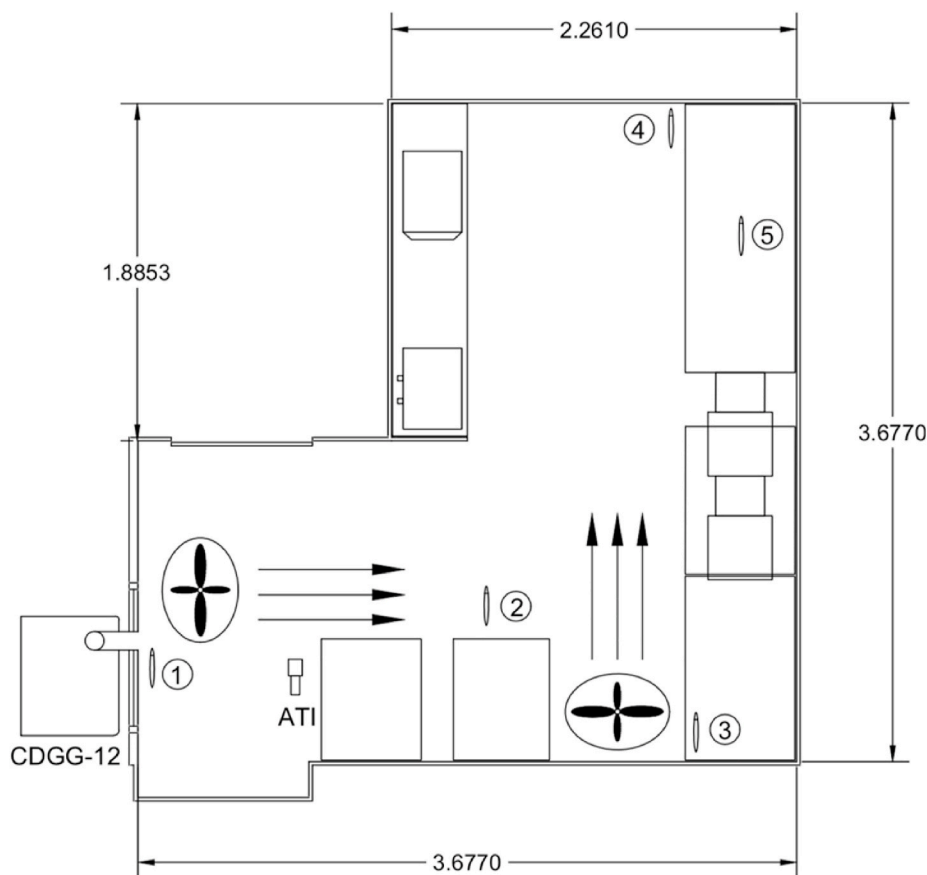


Fig. 3. Schematic diagram of the test room.

In the disinfection experiment, the operational condition was set by two-stage gas flowrates for low and high C_T values at constant Q_L of 0.225 L/min, ω of 1500 rpm, and a total of 265 min. At the first stage of the experiment, the $Q_G = 620$ L/min, at which the outlet ClO_2 concentration from the RPB was 361 ppm, was selected for a low C_T experiment over 140 min. Then, the high C_T experiment was conducted at Q_G value of 192 L/min with the outlet ClO_2 concentration of 1161 ppm from the RPB for the next 125 min.

The fresh air outside the test room was used to strip the ClO_2 solution then injected into the closed room. Five positions for *E. coli* (1, 3, and 5) and biological indicator placement (1, 2, 3, 4, and 5) was shown in Fig. 3. During the disinfection period, the ambient condition of the room was monitored at 30 ± 2 °C. The relative humidity of the room was around 70% before the experiment and increased to 80–85% after the test. The gaseous ClO_2 was measured and recorded every 5 min by the ATI ClO_2 Detector device during the operation time of RPB and afterward until the remaining gaseous ClO_2 concentration reached the minimum level.

3. Results and discussions

3.1. ClO_2 Stripping experiment

3.1.1. Effect of initial concentration (C_{Li})

The effect of C_{Li} (160–1730 mg/L) on the stripping efficiency (η) at the Q_G of 247 L/min, Q_L of 0.084 L/min, and $\omega = 1200$ rpm were presented in Fig. 4. The η values were $99.69 \pm 0.04\%$ and $99.69 \pm 0.02\%$ with the C_{Li} of 160 mg/L and 976 mg/L, respectively. The η slightly reduced to $99.60 \pm 0.03\%$ and $99.57 \pm 0.03\%$ at the higher C_{Li} of 1215 mg/L and 1730 mg/L, respectively. Note that the experimental parameters for RPB stripping are similar to previous works for ammonia (Yuan

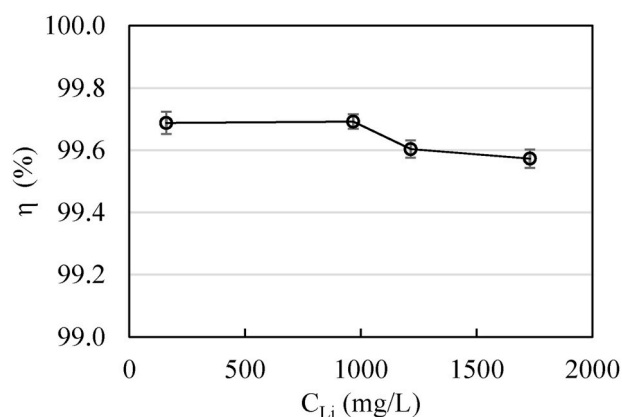


Fig. 4. Effect of C_{Li} on η ($Q_G = 247$ L/min, $Q_L = 0.084$ L/min, $\omega = 1200$ rpm, $T = 30$ °C).

et al., 2016a, b) and isopropyl alcohol (Viet, 2020). The obtained stripping efficiency for ClO_2 with such narrow range can be attributed to its low boiling point (11 °C) and relatively high Henry constant (0.047696) in comparison to their Henry constant of ammonia (0.0008582) and isopropyl alcohol (0.00046378) at 30 °C. The small deviation of all conditions (0.02–0.04%) might be the reflection of the fast-reaching equilibrium of the stripping process by the RPB after 15 min of operation.

The effect of C_{Li} to ClO_2 stripping via RPB was likely negligible since the variation of η with changing of C_{Li} in the experiments was only 0.12%. Regarding the conventional packed column for the stripping process, either a higher Q_G/Q_L ratio or a longer hydraulic retention time

is required to achieve the desired stripping efficiency at higher C_{Li} . In this case of RPB, the Q_G/Q_L ratio for various C_{Li} was constant with a very short hydraulic retention time (<4 s). Therefore, the negligible effect of the C_{Li} on ClO_2 stripping could be the result of a high Q_G/Q_L ratio and high gravitational field which enlarged the mass transfer rate of the process.

3.1.2. Effect of gas-liquid flow rate (Q_G/Q_L) ratio

The effect of Q_G/Q_L ratios and ω on the η value and K_{La} of ClO_2 stripping at $Q_L = 0.092$ L/min is presented in Fig. 5. With the range of Q_G/Q_L ratio from 1000 to 10000, the η values were varied above 98%. As described previously, this outcome would be reasonable since ClO_2 has a low boiling point of 11 °C and a high value of dimensionless Henry constant (0.04770). Also, it should be noted that the higher Q_G/Q_L ratio and faster ω facilitate the enhancement of η and K_{La} .

The results indicated that increasing Q_G exhibits higher η and K_{La} because of the higher stripping factor (S) by supplying a higher amount of fresh air. At $\omega = 900$ rpm, the value of η increased from $98.22 \pm 0.13\%$ to $99.33 \pm 0.05\%$, corresponding to K_{La} improved from $0.00847 \pm 1.6 \times 10^{-4} s^{-1}$ to $0.01042 \pm 1.7 \times 10^{-4} s^{-1}$ at the Q_G/Q_L from 1000 to 10000. Faster rotating speed also showed minor effects in η and K_{La} when these values were marginally increased by 1.2% (from $98.23 \pm 0.13\%$ to $99.44 \pm 0.04\%$) and $0.00244 s^{-1}$ (from $0.00847 \pm 1.6 \times 10^{-4} s^{-1}$ to $0.01013 \pm 1.5 \times 10^{-4} s^{-1}$), respectively, as the ω increased from 900 to 1500 rpm at $Q_G/Q_L = 1000$. It was noticed that higher Q_G/Q_L and faster ω could compensate the deviation rate in η by exhibiting a more stable stripping process. Nevertheless, the deviation could be negligible throughout this experiment. Comparing to the results of ammonia stripping via RPB (Yuan et al., 2016a), at the same condition of the temperature of 30 °C and ω of 900 rpm, η and K_{La} toward ClO_2 stripping

at $Q_G/Q_L = 1000$ (98.23% and $0.00847 s^{-1}$) was significantly higher than that of ammonia stripping at $Q_G/Q_L = 1200$ (approximately 53% and $0.0024 s^{-1}$). The excellent efficiency and mass transfer in ClO_2 stripping could be the result of its physical properties mentioned above.

3.1.3. Effect of liquid flow rate (Q_L)

The effect of Q_L (0.040–0.210 L/min) on η and K_{La} of ClO_2 stripping at Q_G of 494 L/min and 988 L/min and ω of 900 rpm–1500 rpm is presented in Figs. 6 and 7. The η slowly went down with Q_L at both Q_G of 494 L/min and 988 L/min, but the K_{La} increased significantly with higher Q_L . At ω of 900 rpm, with Q_L from 0.040 to 0.210 L/min, the η value slightly dropped from $99.64 \pm 0.04\%$ to $97.43 \pm 0.25\%$ ($Q_G = 494$ L/min) and $99.70 \pm 0.03\%$ to $98.26 \pm 0.15\%$ ($Q_G = 988$ L/min) while the K_{La} was multiplied approximately 3 times ($0.00508 \pm 0.9 \times 10^{-4} s^{-1}$ to $0.01746 \pm 4.7 \times 10^{-4} s^{-1}$ at $Q_G = 494$ L/min, $0.00604 \pm 1.0 \times 10^{-4} s^{-1}$ to $0.01870 \pm 3.9 \times 10^{-4} s^{-1}$ at $Q_G = 988$ L/min). Again, the higher Q_L , which corresponded to lower Q_G/Q_L , led to larger deviation of η data. This event was a result of the disturbance from the large liquid feeding to the RPB leading to the unstable stripping process. At faster ω , the decreasing trend of η was less significant, with only 0.5% and 0.3% decrease of η , but the increasing rate of K_{La} was higher up to 4 times increment ($0.00659 \pm 0.9 \times 10^{-4} s^{-1}$ to $0.02570 \pm 4.4 \times 10^{-4} s^{-1}$ and $0.00766 \pm 0.1 \times 10^{-4} s^{-1}$ to $0.02625 \pm 4.8 \times 10^{-4} s^{-1}$) when the Q_L increased from 0.040 L/min to 0.210 L/min at ω of 1500 rpm. Yuan et al. explained this pattern is caused by the compensatory effect of higher Q_L which resulted in the decrease of liquid retention time and stripping factor leading to lower stripping efficiency (Yuan et al., 2016b). The opposite trend of increasing K_{La} , however, reflected the separation efficiency over time since more liquid fed in the system means a higher mass of ClO_2 is transferred to the gas phase.

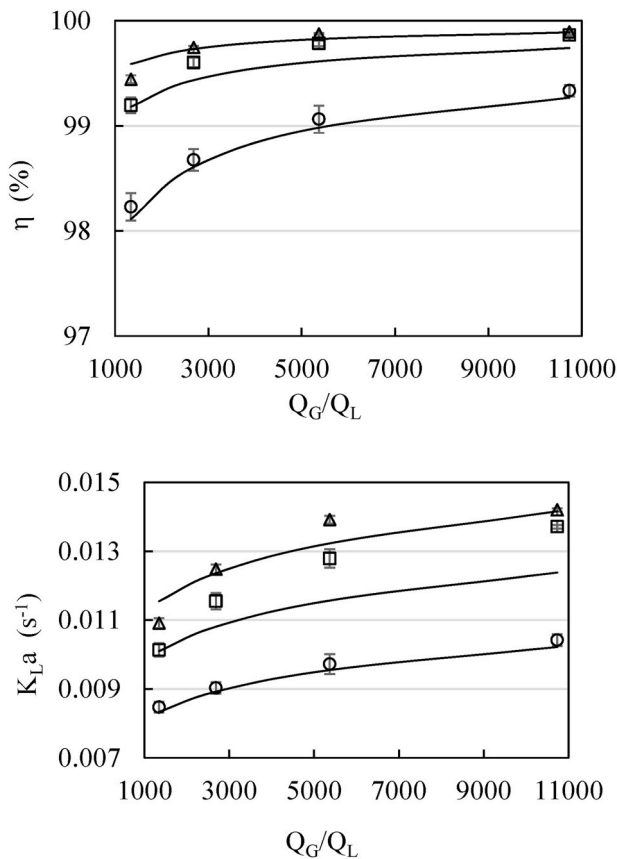


Fig. 5. Effect of Q_G/Q_L ratio on η and K_{La} ($C_{Li} = 1215$ mg/L, $Q_L = 0.092$ L/min, $T = 30$ °C). Symbols: $\omega = 900$ (○), $\omega = 1200$ (□), and 1500 (△) rpm. Solid lines: predictions for η and K_{La} .

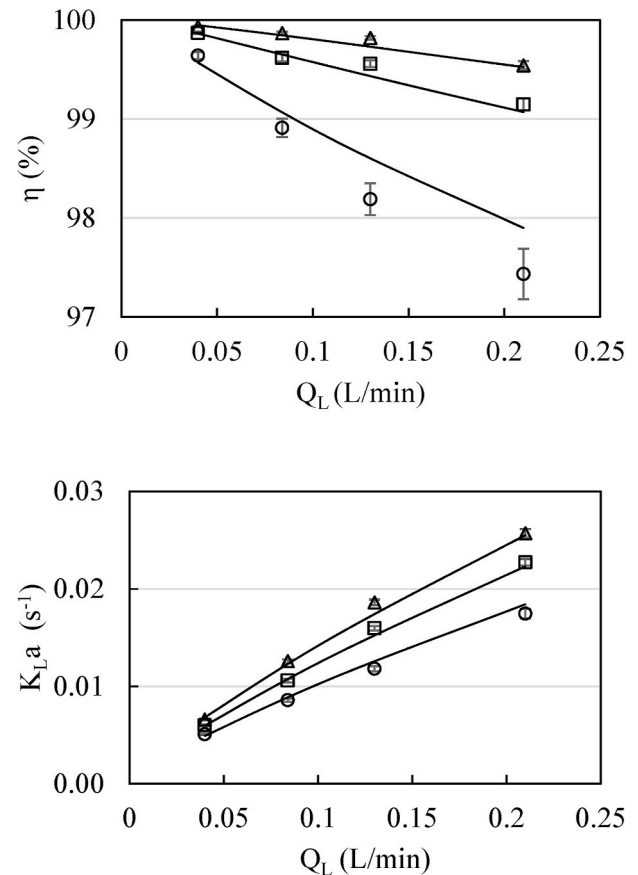


Fig. 6. Effect of Q_L on η and K_{La} at $Q_G = 494$ L/min ($C_{Li} = 1730$ mg/L, $T = 30$ °C). Symbols: $\omega = 900$ (○), $\omega = 1200$ (□), and 1500 (△) rpm. Solid lines: predictions for η and K_{La} .

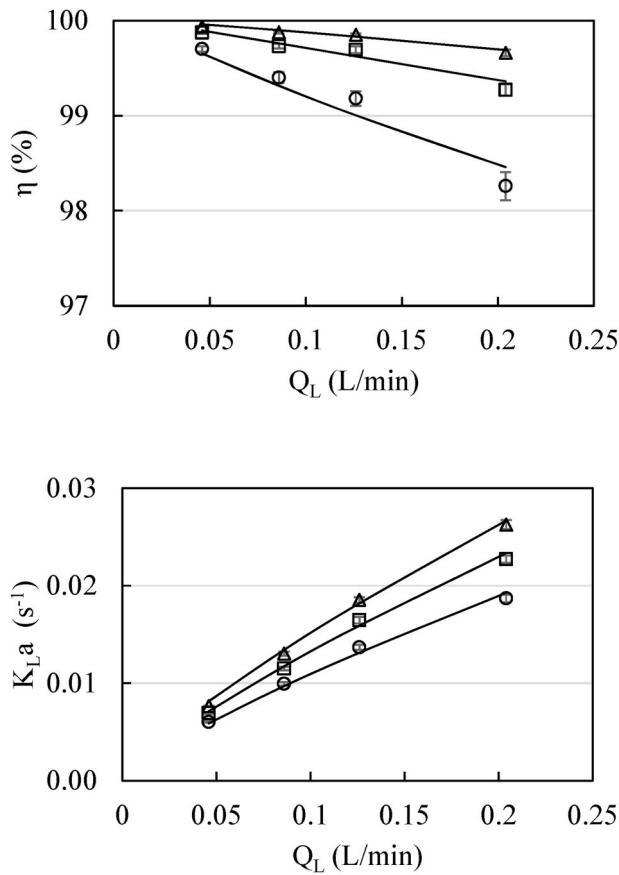


Fig. 7. Effect of Q_L on η and K_La at $Q_G = 988$ L/min ($C_{Li} = 1730$ mg/L, $T = 30$ °C). Symbols: $\omega = 900$ (○), $\omega = 1200$ (□), and 1500 (△) rpm. Solid lines: predictions for η and K_La .

3.2. Comparison of experimental and prediction results

3.2.1. Prediction model for C_G

The ClO_2 concentration in the outlet gas phase (C_G) was theoretically calculated based on the mass balance between liquid and gas phase (Eq. (2)) and the stripping efficiency of the process (Eq. (4)) into Eq. (12) as follows:

$$C_G = \frac{\eta \times C_{Li} \times Q_L}{Q_G} \left(\frac{g}{m^3} \right) \times \frac{24.5 \text{ L}}{67.45 \text{ mol}} \times 1000000 (\text{ppm}) \quad (12)$$

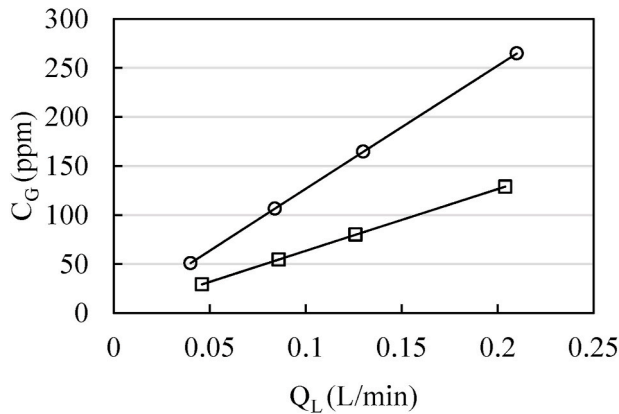


Fig. 8. Effect of Q_L on the outlet gaseous ClO_2 concentration ($C_{Li} = 1730$ mg/L, $\omega = 1200$ rpm). Symbols: $Q_G = 494$ L/min (○), $Q_G = 988$ L/min (□), Solid lines: predictions for C_G .

As shown in Fig. 8, the C_G value from the experiment and from the prediction model has a good agreement. At Q_L from 0.040 to 0.200 L/min, the C_G values at $Q_G = 494$ L/min (50–265 ppm) was about 2 times higher than the corresponding data in $Q_G = 988$ L/min (29–129 ppm) since the doubled amount of fresh air diluted the generated ClO_2 concentration from the constant Q_L condition. According to the experiment and simulation results, the outlet dosage of gaseous ClO_2 as a fumigant from the RPB can be adjusted by either adjusting the Q_L or selecting the different C_{Li} of the ClO_2 solution.

3.2.2. Prediction models for K_La and η

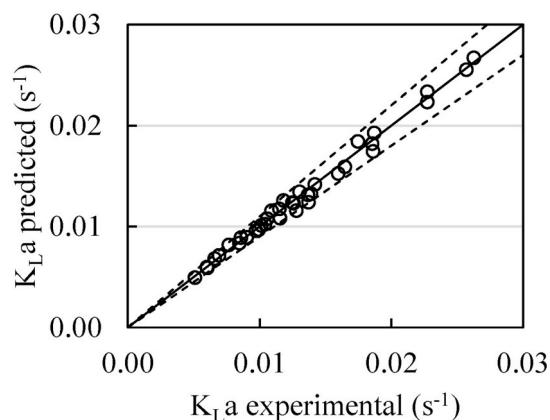
The K_La and η from the stripping process using RPB have been empirically estimated based on the operating variables such as Q_G , Q_L , and ω . According to Liu et al. (1996), Chen and Liu (2002), and Chen et al. (2004), the prediction model for ethanol and VOCs stripping using RPB was developed based on the dimensionless group of Re_L , Re_G , and $Gr_{L,avg}$, by plotting the linear regression of the natural logarithm. The predicted equation ($R^2 = 0.990$) is expressed as follow:

$$\frac{K_L a d_p}{D_L a_p} = 0.394 Re_L^{0.796} Re_G^{0.098} Gr_{L,avg}^{0.305} \quad (13)$$

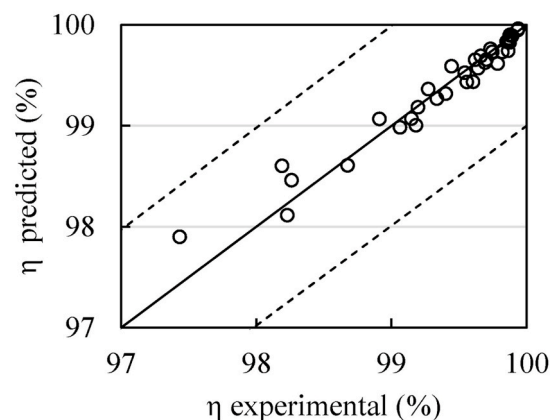
where d_p is the stainless-steel wire diameters of the packing (0.22), a_p is the specific area of packing per unit volume of the packed bed ($840 \text{ m}^2/\text{m}^3$). The D_L value is the molecular liquid diffusion coefficient of ClO_2 at 30 °C ($1.43 \times 10^{-5} \text{ m}^2/\text{s}$). The range of the dimensionless groups in Eq. (12) are $0.09 < K_L a d_p / D_L a_p < 0.49$, $6.55 \times 10^{-5} \ll Re_L < 3.44 \times 10^{-4}$, $1.01 \times 10^{-4} < Re_G < 8.07 \times 10^{-4}$, and $8.10 \times 10^9 < Gr_{L,avg} < 2.36 \times 10^{10}$. According to Eq. (13), the K_La of ClO_2 stripping was mostly driven by the Re_L , and then the $Gr_{L,avg}$ rather than the Re_G , which was in contrast to the case of ammonia stripping where the K_La is sensitive to the Re_G (Yuan et al., 2016a, b). This was also demonstrated in the previous results when the fluctuations of K_La and η were only 0.002 s^{-1} and 1%, respectively. From the predicted K_La values, the corresponded values of η were computed from Eq. (11). The relation between experimental and predicted K_La and η values are presented in Fig. 9. The predicted K_La values completely lie within 10% deviation of the experimental values while the predicted η even complied 1% deviation of the experimental data since it was varied above 97%. The prediction curve derived from Eq. (13) was also been plotted in Figs. 3–6, which showed strong agreement with the results obtained from experiments.

3.3. Disinfection experiment

For the disinfection experiment, the change of gaseous ClO_2 concentration (C_G) over time is shown in Fig. 10. At the first stage of the experiment, the value $Q_G = 620$ L/min over 140 min, at which the outlet ClO_2 concentration from the RPB was 361 ppm, was conducted. At the first 70 min, the C_G in the room rapidly increased from 0 to 105.3 ppm, which is significantly faster than the period of 2 h to reach 40 ppm by acid-chlorite reaction method (Shirasaki et al., 2016). Comparing to the commercial equipment, the generation speed and dosage in this experiment were slower than the CD cartridge using chlorine-chlorite mechanism (1800 ppm after 20 min) (Eylath et al., 2003). The higher dosage from the RPB stripping equipment can be enhanced by either a higher concentration of input ClO_2 solution or higher input liquid flow rate or even both. The rapid increment then idled as there was only almost 15 ppm of increase in the next 70 min. The reason for this phenomenon might be the dilution effect since the fresh air from outside of the closed room was used for the stripping of the ClO_2 solution. Therefore, the lower Q_G value of 192 L/min with the outlet ClO_2 concentration of 1161 ppm from the RPB was adopted to overcome the dilution effect and generate a higher C_T value in the second stage from the period of 140–260 min. The results indicated that the C_G was gradually improved and reached the highest value in the room of 151.4 ppm at 260 min. The C_G then dropped significantly by 125 ppm (to 24.6 ppm) from 260 min



(a)



(b)

Fig. 9. Diagonal graph of experimental and predicted (a) K_{La} and (b) η . Solid lines: Predictions for K_{La} and η were based on Eqs. 10 and 12, respectively. Dotted lines: Prediction values within (a) $\pm 10\%$ and (b) $\pm 1\%$.

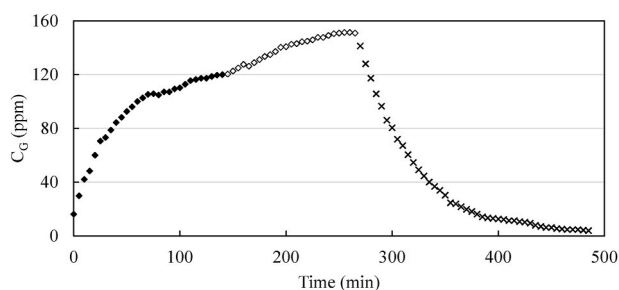








Fig. 10. Generation of gaseous ClO_2 using the RPB in the test room (30.6 m^2), operating condition: $Q_L = 0.255 \text{ L/min}$; $Q_G = 620$ (\blacklozenge), 192 L/min (\diamond), off (\times); $\omega = 1500 \text{ rpm}$; $C_{Li} = 2431 \text{ mg/L}$.

to 355 min after the RPB was shut down. The residual gaseous ClO_2 then gradually diffused in the room for more than 2 h to the lowest point of 3.9 by the end of the experiment.

The result of disinfection efficiency toward *E. coli* and *G. stearothermophilus* bio-indicator is presented in Table 2. Regards to *E. coli*, the gaseous ClO_2 at $C_T = 642 \text{ ppm-h}$ showed a 5 log reduction as completely inactivation of the disk population of 10^5 , 10^4 , and 10^3 at all 5 sites in the room. In the study of Shirasaki et al. (2016), 10^{48} CFU/disk of *E. coli* was completely inactivated only with 10 ppm after 24 h ($C_T = 240 \text{ ppm-h}$). It indicated that the dosage of ClO_2 in this research was at an exceeding required amount for *E. coli* disinfection. This approximate

Table 2

Disinfection efficiency of *E. coli* and *G. stearothermophilus* by ClO_2 from RPB.

$C_T = 642 \text{ ppm-h}$, $C_{G,avg} = 78.7 \text{ ppm}$, $\text{RH} = 81\%$				
Site	Bacteria	Log reduction	Indicator	Disinfection Efficiency (%)
1	<i>E. coli</i>	5		100
	<i>G. stearothermophilus</i>	6 (no growth)		100
2	<i>G. stearothermophilus</i>	6 (no growth)		100
3	<i>E. coli</i>	5		100
	<i>G. stearothermophilus</i>	4 (slightly growth)		99.99
4	<i>G. stearothermophilus</i>	4 (slightly growth)		99.99
5	<i>E. coli</i>	5		100
	<i>G. stearothermophilus</i>	3 (growth)		99.9
Control	<i>G. stearothermophilus</i>	0 (Fully growth)		0

C_T value of ClO_2 was also achieved in the research of Lowe et al. (2013), at which they found 9.96 of mean log reduction of *E. coli* at C_T of 677 ppm-h. However, the uneven distribution of ClO_2 among different sites of the test room was described via the effect on the *G. stearothermophilus* bio-indicator. At sites 1 and 2, where were closest to the injection point, the inactivation capacity showed the excellent result as a 6-log reduction of the spore at which no growth was detected after 8 h of incubation (Table 2). The RPB stripping-based ClO_2 generation obtained a similar inactivation result with the commercial equipment by Lowe et al. (2013) where the *B. atrophaeus* and *E. coli* were also completely inactivated with a similar C_T value of 677 ppm-h and humidity of 50%.

The inactivation effects were also observed from the sites of 3–5. According to the color indication, there was a slight growth on the *G. stearothermophilus* where the log reduction was recorded at 4 (99.99% inactivation) in sites 3 and 4. The lowest inactivation was observed to be at the farthest corner of the room to the injection point at which site 5 only showed only 3 log reduction of the spores (99.9% inactivation) and the sight of growth after 8-h incubation. According to Lorcheim (2017), the suggested C_T value and humidity for 6-log kill toward spores is 600 ppm-h and 65%, respectively. Since the current study only monitored the C_T value near sites 1 and 2, the C_T values of other farther sites would be low. Therefore, an uneven distribution of gaseous ClO_2 between sites was expected leading to lower C_T at sites 3, 4, and 5. Nevertheless, this issue can be resolved by improving the air circulation method in the test room during the ClO_2 stripping via RPB.

It should be pointed out that two experimental factors can be encouraged to be considered in future on-site disinfection tests for a better performance evaluation of C_T effect. Firstly, multiple concentration profiles of ClO_2 from each site would be decisive to evaluate the effect of C_T on the inactivation of biological indicators. Since the testing lab must be completely closed and sealed to prevent the leakage of gaseous ClO_2 during the long-term experiment, multiple monitors should be adopted if possible. Further, the effect of C_T on different modes of air circulation in the testing room would be also worthily examined for developing the protocol for disinfection and sterilization in medical or healthcare facilities.

4. Conclusions

In this study, the feasibility of using an RPB as an intensified stripper for a non-chemical-reaction ClO_2 generation was demonstrated. The effervescent tablet method was adopted to produce ClO_2 and simultaneously strip out to avoid the expected decay in ClO_2 solution concentration. The obtained results indicated that the gaseous ClO_2 can be effectively and rapidly generated via a fully controlled physical process with the input material of commercially abundant ClO_2 solution. The

stripping efficiency of ClO_2 ranged above 97% and invulnerable from the change of C_{Li} (100–2000 mg/L) and Q_{L} (0.04–0.250 L/min). According to the experimental results and empirical model, the overall K_{La} rather depends on the change of Q_{L} and ω than Q_{G} , and was significantly higher ($0.009\text{--}0.027\text{ s}^{-1}$) than other target compounds via RPB stripping. Within the scale of this experiment, the C_{G} of ClO_2 can be predicted and adjusted from 10 ppm to over 1000 ppm by the established prediction model with controlling C_{Li} , Q_{L} , Q_{G} and ω . The results of the on-site disinfection test in the *Mycobacterium Tuberculosis* Laboratory have shown effective elimination of all sites of *E. coli* and 2 of 5 sites of *G. stearothermophilus* with a C_{T} value at the gas monitoring point of 642 ppm-h and humidity of 81%. The findings indicated an outstanding mass transfer and efficiency in transferring ClO_2 from the liquid phase to the fumigant form via a non-chemical reaction process without related safety concerns from gas tank storage and handling. Throughout the process, the parameter adjustment of the compacted and all-in-one RPB system is rapid and highly user-friendly to continuously generate gaseous ClO_2 . Although this study has carefully controlled the C_{T} value (i.e., the exposure gaseous concentration at a certain contacting period) with two-stage flow experiments and found similar inactivation outcomes with previous studies, more efforts should be encouraged on the effect of various C_{T} at each site, different modes of air circulation, and distances from the injection point to the inactivation efficiency in a testing room for ClO_2 sterilization in medical or healthcare sectors.

CCRediT author contribution statement

Viet Minh Trinh: performed the experiments, Formal analysis, Writing – original draft, revised the paper. **Min-Hao Yuan:** discussed the results and provided suggestion, Writing – original draft, revised the paper. **Yi-Hung Chen:** conceived and designed the experiments, contributed reagents/materials/analysis tools, discussed the results and provided suggestion, Writing – original draft, revised the paper. **Chen-Yang Wu:** performed the experiments, Formal analysis. **Shao-Chi Kang:** performed the experiments, Formal analysis. **Pen-Chi Chiang:** conceived and designed the experiments, contributed reagents/materials/analysis tools, discussed the results and provided suggestion, revised the paper. **Han-Pang Huang:** conceived and designed the experiments, contributed reagents/materials/analysis tools. **Yu-Lin Zhao:** performed the experiments, Formal analysis. **Ji-Fan Lin:** contributed reagents/materials/analysis tools, discussed the results and provided suggestion. **Chien-Hsien Huang:** Conceptualization, and designed the experiments, contributed reagents/materials/analysis tools. **Jiann-Horng Yeh:** conceived and designed the experiments; contributed reagents/materials/analysis tools. **Der-Ming Lee:** performed the experiments; contributed reagents/materials/analysis tools.

Declaration of competing interest

The authors declare that they have no known competing financial interests or personal relationships that could have appeared to influence the work reported in this paper.

Acknowledgements

This work is supported by the Ministry of Science and Technology, Taiwan [108-2622-E-027-005-CC3 and 108-2221-E-027-073-MY3].

References

- Chen, Y.-S., Liu, H.-S., 2002. Absorption of VOCs in a rotating packed bed. *Ind. Eng. Chem. Res.* 41 (6), 1583–1588.
- Chen, Y.H., Chang, C.Y., Su, W.L., Chen, C.C., Chiu, C.Y., Yu, Y.H., Chiang, P.C., Chiang, S.I.M., 2004. Modeling ozone contacting process in a rotating packed bed. *Ind. Eng. Chem. Res.* 43 (1), 228–236.
- Chen, Y.-S., Lin, C.-C., Liu, H.-S., 2005a. Mass transfer in a rotating packed bed with various radii of the bed. *Ind. Eng. Chem. Res.* 44 (20), 7868–7875.
- Chen, Y.-S., Lin, C.-C., Liu, H.-S., 2005b. Mass transfer in a rotating packed bed with viscous Newtonian and non-Newtonian fluids. *Ind. Eng. Chem. Res.* 44 (4), 1043–1051.
- Chen, T.-L., Chen, Y.-H., Zhao, Y.-L., Chiang, P.-C., 2020. Application of gaseous ClO_2 on disinfection and air pollution control: a mini review. *Aerosol and Air Quality Research* 20 (11), 2289–2298.
- Cortes Garcia, G.E., van der Schaaf, J., Kiss, A.A., 2017. A review on process intensification in HiGee distillation. *Journal of Chemical Technology & Biotechnology* 92 (6), 1136–1156.
- Eylath, A., Wilson, D.L., Thatcher, D.R., Pankau, A., 2003. Successful Sterilization Using Chlorine Dioxide Gas Part One : Sanitizing an Aseptic Fill Isolator.
- Gudena, K., Rangaiah, G.P., Lakshminarayanan, S., 2011. Optimal design of a rotating packed bed for VOC stripping from contaminated groundwater. *Ind. Eng. Chem. Res.* 51 (2), 835–847.
- Jeng, D.K., Woodworth, A.G., 1990. Chlorine dioxide gas sterilization under square-wave conditions. *Appl. Environ. Microbiol.* 56 (2), 514–519.
- Jiang, D.L., Chen, B.W., Ni, G.W., 2012. Application of chlorine dioxide in drinking water disinfection. *Adv. Mater. Res.* 461, 497–500.
- Jiang, X., Rayner, S., Luo, M.H., 2020. Does SARS-CoV-2 has a longer incubation period than SARS and MERS? *J. Med. Virol.* 92 (5), 476–478.
- Kelleher, T., Fair, J.R., 1996. Distillation studies in a high-gravity contactor. *Ind. Eng. Chem. Res.* 35 (12), 4646–4655.
- Khan, M.H., Yadav, H., 2020. Sanitization during and after COVID-19 pandemic: a short review. *Transactions of the Indian National Academy of Engineering* 5 (4), 617–627.
- Li, J., Jin, R., Cheng, S., 2012. Research status and application of solid chlorine dioxide. *Chemical Intermediate* 9 (1), 44–47.
- Lin, C.-C., Liu, W.-T., Tan, C.-S., 2003. Removal of carbon dioxide by absorption in a rotating packed bed. *Ind. Eng. Chem. Res.* 42 (11), 2381–2386.
- Liu, H.-S., Lin, C.-C., Wu, S.-C., Hsu, H.-W., 1996. Characteristics of a rotating packed bed. *Ind. Eng. Chem. Res.* 35 (10), 3590–3596.
- Lorchheim, K., 2017. Principles of chlorine dioxide gas as a decontamination method. <http://www.clordisys.com/pdfs/conference/Kevin%20Lorchheim%20-%20Principles%20of%20CD%20Gas.pdf>. Accessed January 22nd 2021.
- Lowe, J.J., Gibbs, S.G., Iwen, P.C., Smith, P.W., Hewlett, A.L., 2013. Impact of chlorine dioxide gas sterilization on nosocomial organism viability in a hospital room. *Int J Environ Res Public Health* 10 (6), 2596–2605.
- Lu, M.-C., Chen, P.-L., Huang, D.-J., Liang, C.-K., Hsu, C.-S., Liu, W.-T., 2021. Disinfection efficiency of hospital infectious disease wards with chlorine dioxide and hypochlorous acid. *Aerobiologia* 37 (1), 29–38.
- NIST chemistry WebBook. <https://webbook.nist.gov/cgi/cbook.cgi?Name=ClO2&Units=SI>.
- Okamoto, K., Rhee, Y., Schoeny, M., Lolans, K., Cheng, J., Reddy, S., Weinstein, R.A., Hayden, M.K., Popovich, K.J., 2019. Impact of doffing errors on healthcare worker self-contamination when caring for patients on contact precautions. *Infection control and hospital epidemiology* 40 (5), 559–565.
- Ran, Y., Qingmin, C., Maorun, F., 2019. Chlorine dioxide generation method and its action mechanism for removing harmful substances and maintaining quality attributes of agricultural products. *Food Bioprocess Technol.* 12 (7), 1110–1122.
- Shirasaki, Y., Matsuura, A., Uekusa, M., Ito, Y., Hayashi, T., 2016. A study of the properties of chlorine dioxide gas as a fumigant. *Experimental animals* 65 (3), 303–310.
- Singh, S.P., Wilson, J.H., Counce, R.M., Lucero, A.J., Reed, G.D., Ashworth, R.A., Elliott, M.G., 1992. Removal of volatile organic compounds from groundwater using a rotary air stripper. *Ind. Eng. Chem. Res.* 31 (2), 574–580.
- Suman, R., Javaid, M., Haleem, A., Vaishya, R., Bahl, S., Nandan, D., 2020. Sustainability of coronavirus on different surfaces. *J Clin Exp Hepatol* 10 (4), 386–390.
- Trinetta, V., Vaidya, N., Linton, R., Morgan, M., 2011. Evaluation of chlorine dioxide gas residues on selected food produce. *J. Food Sci.* 76 (1), T11–T15.
- US-EPA. EPA on-line tools for site assessment calculation. <https://www3.epa.gov/ceampub/learn2model/part-two/onsite/estdiffusion-ext.html>. (Accessed 17 January 2021). Accessed.
- Viet, T.M., 2020. Air Stripping of Aqueous Solution Containing IPA, Ammonia and ClO_2 Using Rotating Packed Beds, Institute of Chemical Engineering. National Taipei University of Technology, Taipei, Taiwan.
- Wang, Q., Chen, K., Li, J., Xu, J., Liu, S., 2011. Simultaneous determination of chlorine dioxide and hypochlorous acid in bleaching system. *Bioresources* 6.
- WHO, 2020. WHO Director-General's opening remarks at the media briefing on COVID-19 - 20 March 2020 (Accessed March 14th 2020). <https://www.who.int/director-general/speeches/detail/who-director-general-s-opening-remarks-at-the-media-briefing-on-covid-19-20-march-2020>.
- Yuan, M.-H., Chen, Y.-H., Tsai, J.-Y., Chang, C.-Y., 2016a. Ammonia removal from ammonia-rich wastewater by air stripping using a rotating packed bed. *Process Saf. Environ. Protect.* 102, 777–785.
- Yuan, M.-H., Chen, Y.-H., Tsai, J.-Y., Chang, C.-Y., 2016b. Removal of ammonia from wastewater by air stripping process in laboratory and pilot scales using a rotating packed bed at ambient temperature. *Journal of the Taiwan Institute of Chemical Engineers* 60, 488–495.
- Zhang, M., 2011. Instant chlorine dioxide effervescent tablet and preparation method thereof. China.
- Zhao, Y., Xin, H., Zhao, D., Zheng, W., Tian, W., Ma, H., Liu, K., Hu, H., Wang, T., Soupir, M., 2014. Free chlorine loss during spraying of membraneless acidic electrolyzed water and its antimicrobial effect on airborne bacteria from poultry house. *Ann. Agric. Environ. Med. : AAEM* 21 (2), 249–255.

Glossary

RPB: rotating packed bed

C_T : concentration (ppm) of a disinfection in a contact time (h), ppm-h

VOCs: volatile organic compounds

K_{La} : overall liquid volumetric mass transfer coefficient (s^{-1})

r_i : inner radius of a packed bed (m)

r_o : outer radius of a packed bed (m)

r_{avg} : average radius of a packed bed (m)

Z_B : axial height of a packed bed (m)

V_B : volume of a packed bed (m^3)

a_p : specific area of a packing per unit volume of a packed bed (m^2/m^3)

Q_L : liquid flow rate (L/min)

Q_G : gas flow rate (L/min)

Q_G/Q_L : gas-liquid flow rate ratio

ω : rotating speed (rpm or rad/s)

C_{Li} : inlet concentration of ClO_2 in the liquid phase

C_{Lo} : outlet concentration of ClO_2 in the liquid phase

C_G : outlet concentration of ClO_2 in the gas phase

η : stripping efficiency (%)

H_C : dimensionless Henry's law constant of ClO_2

S : stripping factor

ν_L : dynamic liquid viscosity (m^2/s), 8.01×10^{-7} at $30^\circ C$

ρ_G : gas density (kg/m^3), 1.166 at $30^\circ C$

μ_G : gas viscosity ($kg/m.s$) 1.87 at $30^\circ C$

ρ_L : liquid density (kg/m^3), 998.5 at $30^\circ C$

μ_L : liquid viscosity ($kg/m.s$), 0.798 at $30^\circ C$

D_L : molecular liquid distribution of ClO_2 (m^2/s), 1.43×10^{-5} at $30^\circ C$

d_p : stainless wire diameter of the bed (m), 0.22

$Gr_{L, avg}$: Grashof number of the liquid based on the average bed radius

Re_G : Reynolds number of the gas

Re_L : Reynolds number of the liquid